2.5. ELECTRON DIFFRACTION AND ELECTRON MICROSCOPY IN STRUCTURE DETERMINATION
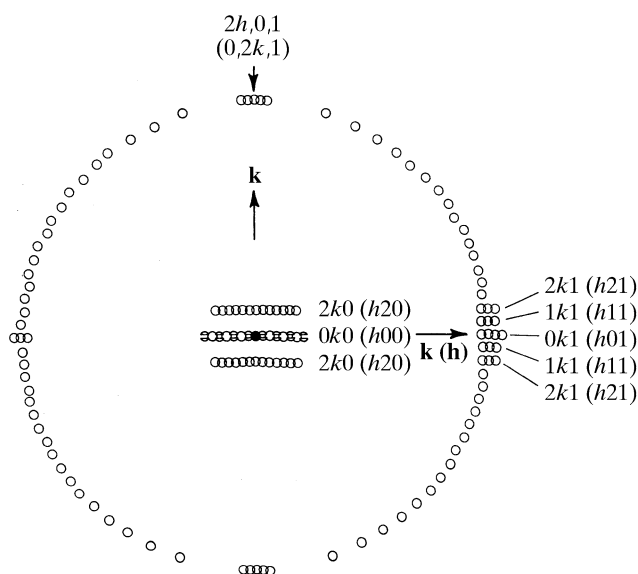


Fig. 2.5.3.3. Diagrammatic representation of the influence of non-symmorphic elements: (i) Alternate rows of the zero-layer pattern are absent owing to the horizontal glide plane. The pattern is indexed as for an 'a' glide; the alternative indices (in parentheses) apply for a 'b' glide. (ii) GS bands are shown along the central row of the zero layer, for odd-order reflections.

inversion symmetry has been resolved recently by Tanaka *et al.* (1994) using both CBED and LACBED techniques.

(ii) *Vertical mirror plane* determination may be the most accurate crystal point-symmetry test, given that it is possible to follow the symmetry through large crystal rotations (say 5 to 15°) about the mirror normal. It is also relatively unaffected by crystal surface steps as compared to (v) below.

(iii) *Horizontal glide planes* are determined unequivocally from zero-layer absences when the first Laue zone is recorded, either with the main pattern or by further crystal rotation; *i.e.* a section of this zone is needed to determine the lateral unit-cell parameters. This observation is illustrated diagrammatically in Fig. 2.5.3.3.

(iv) An extinction (GS) line or band through odd-order reflections of a zone-axis pattern indicates only a *projected glide line*. This is true because both $P2_1$ (No. 4) and $Pa$ (No. 7) symmetries project into '$pg$' in two dimensions. However, the projection approximation has only limited validity in CBED. For all crystal rotations *around* the $2_1$ axis, or alternatively *about the glide-plane 'a' normal*, dynamic extinction conditions are retained. This is summarized by saying that the diffraction vector $K_{0g}$ should be either normal to a screw axis or contained within a glide plane for the generation of the $S$ or $G$ bands, respectively. Hence $P2_1$ and $Pa$ may be distinguished by these types of rotations away from the zone axis with the consequence that the element $2_1$ in particular is characterized by extinctions close to the Laue circle for the tilted ZOLZ pattern (Goodman, 1984*b*), and that the glide $a$ will generate extinction bands through both ZOLZ and HOLZ reflections for all orientations maintaining Laue-circle symmetry about the $S$ band (Steeds *et al.*, 1978).

As a supplement to this, in a refined technique not universally applicable, Tanaka *et al.* (1983) have shown that fine-line detail from HOLZ interaction can be observed which will separately identify $S$- ($2_1$) and $G$-band symmetry from a single pattern (see Fig. 2.5.3.6).

(v) The centre-of-symmetry (or $\pm H$) test can be made very sensitive by suitable choice of diffraction conditions but requires a reasonably flat crystal since it involves a pair of patterns (the angular beam shift involved is very likely to be associated with

some lateral probe shift on the specimen). This test is best carried out at a low-symmetry zone axis, free from other symmetries, and preferably incorporating some $\overline{\text{fine}}$-line HOLZ detail, in the following way. The *hkl* and $\overline{hkl}$ reflections are successively illuminated by accurately exchanging the central-beam aperture with the diffracted-beam apertures, having first brought the zone axis on to the electron-microscope optic axis. This produces the symmetrical $\pm H$ condition.

(vi) In seeking internal $m_R$ symmetry as a test for a horizontal diad axis it is as well to involve some distinctive detail in the mirror symmetry (*i.e.* simple two-beam-like fringes should be avoided), and also to rotate the crystal about the supposed diad axis, to avoid an $m_R$ symmetry due to projection [for examples see Fraser *et al.* (1985) and Goodman & Whitfield (1980)].

(vii) The presence or absence of the in-disc centrosymmetry element $1_R$ formally indicates the presence or absence of a horizontal mirror element $m'$, either as a true mirror or as the mirror component of a horizontal glide plane $g'$. In this case the *absence* of symmetry provides more positive evidence than its presence, since absence is sufficient evidence for a lack of central-mirror crystal symmetry but an observed symmetry could arise from the operation of the projection approximation. If some evidence of the three-dimensional interaction is included in the observation or if three-dimensional interaction (from a large $c$ axis parallel to the zone axis) is evident in the rest of the pattern, this latter possibility can be excluded. Interpretation is also made more positive by extending the angular aperture, especially by the use of LACBED.

These results are illustrated in Table 2.5.3.2 and by actual examples in Section 2.5.3.5.

### 2.5.3.4. *Auxiliary tables*

Space groups may very well be identified using CBED patterns from an understanding of the diffraction properties of real-space symmetry elements, displayed for example in Table 2.5.3.2. It is, however, of great assistance to have the symmetries tabulated in reciprocal space, to allow direct comparison with the pattern symmetries.

There are three generally useful ways in which this can be done, and these are set out in Tables 2.5.3.3 to 2.5.3.5. The simplest of these is by means of point group, following the procedures of Buxton *et al.* (1976). Next, the CBED pattern symmetries can be listed as diperiodic groups which are space groups in two dimensions, allowing identification with a restricted set of three-dimensional space groups (Goodman, 1984*b*). Finally, the dynamic extinctions (GS bands and zero-layer absences) can be listed for each non-symmorphic space group, together with the diffraction conditions for their observation (Tanaka *et al.*, 1983; Tanaka & Terauchi, 1985). Descriptions for these tables are given below.

*Table 2.5.3.3.* BESR symbols (Buxton *et al.*, 1976) incorporate the subscript $R$ to describe reciprocity-related symmetry elements, $R$ being the operator that rotates the disc pattern by 180° about its centre. The symbols formed in this way are $1_R, 2_R, 4_R, 6_R$, where $X_R$ represents $2\pi/X$ rotation about the zone axis, followed by $R$. Of these, $2_R$ represents the $\pm H$ symmetry (two twofold rotations) described earlier [equation (2.5.3.2)] as a transformation of crystalline centrosymmetry; $6_R$ may be thought of as decomposing into $3 \cdot 2_R$ for purposes of measurement. The mirror line $m_R$ (Fig. 2.5.3.2) is similarly generated by $m \cdot 1_R$.

Table 2.5.3.3 gives the BESR interrelation of pattern symmetries with point group (Buxton *et al.*, 1976; Steeds, 1983). Columns I and II of the table list the point symmetries of the whole pattern and bright-field pattern, respectively; column III gives the BESR diffraction groups. [*Note:* following the Pond & Vlachavas (1983) usage, '*' has been appended to the centrosymmetric groups.]

289

references